

Transform Domains

“All mathematics is a language that is well tuned, finely honed, to describe patterns; be it patterns in a star, which has five points that are regularly arranged, be it patterns in numbers like 2, 4, 6, 8, 10 that follow very regular progression.”

Brian Greene (1963-)

The fundamental idea of transforms is to change the way data is represented, i.e. transform the data into a (hopefully more) useful domain, whose properties can be exploited to:

1. make processing easier or computationally more efficient
2. improve the separation or clustering
3. reduce the problem

Ultimately, finding the right domain can make finding patterns in data more easier, even straight forward. The most basic way to change the underlying representation of your data or image is to change the coordinate system representing the data.

5.1 Change of Basis

A coordinate system is simply a choice of basis vectors to represent our data. The linear combination of these basis vectors allows us to represent the entire space of the coordinate system however we wish. Turns out, the choice of coordinate system is not unique and no one coordinate system is universal. This is the fundamental concept behind one of the most successful theories in science - Einstein's Theories of Special and General Relativity.

5.1.1 Basis Vectors

In linear algebra, we can write any vector space via a set of basis vectors $\{e_j\}$, where $j = 1, \dots, n$ and n is the dimension of the space. The basis vectors are generally of length unity and orthogonal to each other.

Orthogonality means the vectors are linearly independent and thus have no common components. We can understand this concept of Orthogonality by understanding the dot product of vectors.

5.1.2 Dot Product

The key idea behind coordinate system basis vectors is the concept of the dot (or inner) product. The dot product $\mathbf{a} \cdot \mathbf{b}$ between the vector \mathbf{a} and vector \mathbf{b} of dimension n can be written as

$$\mathbf{a} \cdot \mathbf{b} = \sum_{j=0}^{n-1} a_j b_j \quad (5.1)$$

If the vectors \mathbf{a} and \mathbf{b} are orthonormal, then $\mathbf{a} \cdot \mathbf{b} = \delta_{ij}$, where δ_{ij} is the Dirac delta function defined as

$$\delta_{ij} = \begin{cases} 0, & i \neq j \\ 1, & i = j. \end{cases} \quad (5.2)$$

For basis vectors, this function simply states that the only vector that has a common component to a vector like e_j is the vector e_j itself.

Thus, we are not limited to conventional coordinate systems and we should in fact change to a coordinate system, i.e. to a new basis set, which is more ‘convenient’ in your scenario. If we ‘transform’ our coordinate system from one to another, we can change our representation. If we change our representation, we might find that our pattern analysis is simplified.

Consider the simple example of data that follows an exponential trend. We could fit an exponential curve or function to the data and that will work fine. However, an exponential is a non-linear function, computing it computationally expensive and it is difficult to plot or visualise because of the growth of values. But if we transform our data into the logarithmic domain, the exponential data becomes linear and the analysis of a line is much simpler!

The problem arises: what representation is ‘best’ to use and how do we find them? This is not an easy question, however there are special types of transforms that a generic tools that can be used for most types of data and this chapter will cover some of them. The first such transform is one based on physical systems and oscillations called the Fourier transform.

5.2 Fourier Transform

The Fourier transform (FT) is the change of basis to a harmonic representation of the data. In other words, we fit trigonometric functions, the so called sines and cosines, to our data to determine the harmonic representation or Fourier space of the data. This transformation is a natural process and consequence of complex numbers and traversing a unit circle.

5.2.1 Unit Circle

A complex number $z = x + iy$ with $i^2 = -1$ can also be written in polar coordinates as

$$z = re^{i\theta}. \quad (5.3)$$

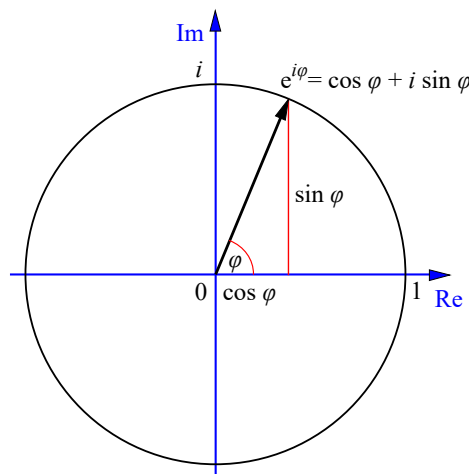


Figure 5.1: Euler's formula for the complex number $z = x + iy$ so that $e^{i\theta} = \cos \theta + i \sin \theta$ and $z = re^{i\theta}$.

This is Euler's formula and is shown in figure 5.1. Multiplying two complex numbers ($z_1 = r_1 e^{i\theta}$ and $z_2 = r_2 e^{i\phi}$) of unit length is therefore equivalent to rotating around the unit circle

$$z = z_1 \cdot z_2 \quad (5.4)$$

$$= r_1 e^{i\theta} \cdot r_2 e^{i\phi} \quad (5.5)$$

$$= r_1 r_2 e^{i(\theta+\phi)} \quad (5.6)$$

$$= e^{i(\theta+\phi)}. \quad (5.7)$$

This is the same as adding the angles of the two vectors together and since the length is unity, this results in the vector z_1 rotating around the origin by an additional ϕ radians or vice versa for z_2 .

5.2.2 Roots of Unity

The data that we usually deal with is discretised, i.e. we have a fixed number of samples. If this is of a physical system like a ball being thrown under the influence of Earth's gravity, it might represent a fixed number of samples of the ball position in space. However, the ball follows a perfect parabolic trajectory when ignoring air resistance, but our samples represent snapshots of this trajectory over time.

In discrete Fourier analysis, we study the rate that our data oscillates around the unit circle. Therefore, if we have N sample points, we usually divide the circle into N equal parts. This division of the circle is algebraically known as the N th root of unity $\omega = e^{2\pi i/N}$. You can show that by traversing around the unit circle with each N th root of unity steps, one will trace out a sine or cosine curve depending on starting position. The rate at which you traverse the unit circle (perhaps by multiples of ω) will trace out sine curves of different frequencies.

5.2.3 Harmonics

The harmonics are then just traversals of the unit circles at different rates of the root of unit ω . Traversing the unit circle and tracing the resulting point over time will reveal of sine curve. If one traverses and traces

out every point corresponding to an angle caused by the root of unit ϕ_ω starting from the point (1,0), we will get a sine curve with a wavelength of 1. Figure 5.2 shows the various harmonics generated by traversing the unit circle by every increasing rates of multiples of ω .

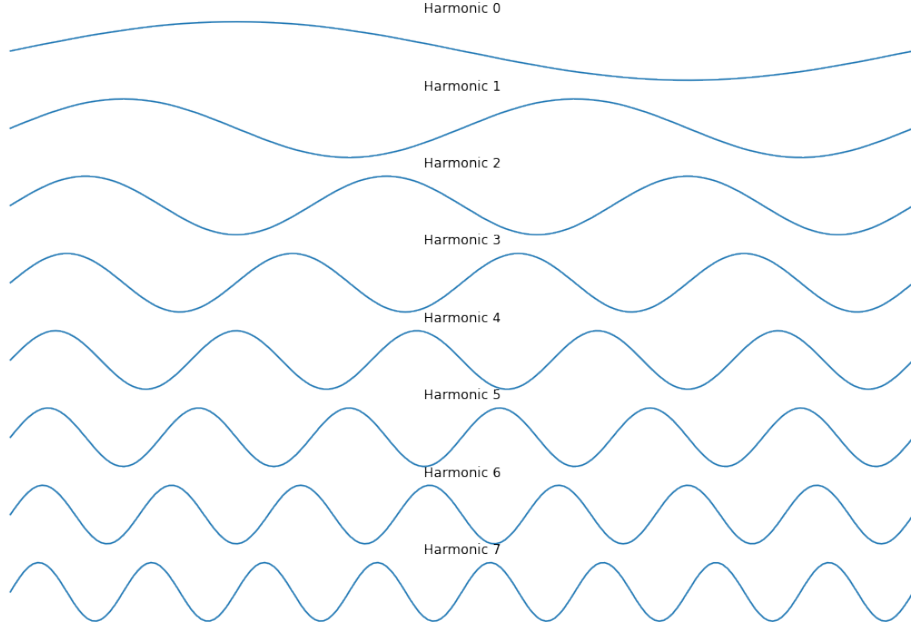


Figure 5.2: Each harmonic $n - 1$ that results from traversing the unit circle at the rate ω^n .

To visualise this process for $N = 8$, consider the construction of a matrix with each row representing different rates of unit circle traversal, which is equivalent to different powers of ω . We get the following Fourier matrix

$$\mathbf{F} = \begin{bmatrix} \omega^0 & \omega^0 & \omega^0 & \omega^0 & \omega^0 & \omega^0 & \omega^0 & \omega^0 \\ \omega^0 & \omega^1 & \omega^2 & \omega^3 & \omega^4 & \omega^5 & \omega^6 & \omega^7 \\ \omega^0 & \omega^2 & \omega^4 & \omega^6 & \omega^8 & \omega^{10} & \omega^{12} & \omega^{14} \\ \omega^0 & \omega^3 & \omega^6 & \omega^9 & \omega^{12} & \omega^{15} & \omega^{18} & \omega^{21} \\ \omega^0 & \omega^4 & \omega^8 & \omega^{12} & \omega^{16} & \omega^{20} & \omega^{24} & \omega^{28} \\ \omega^0 & \omega^5 & \omega^{10} & \omega^{15} & \omega^{20} & \omega^{25} & \omega^{30} & \omega^{35} \\ \omega^0 & \omega^6 & \omega^{12} & \omega^{18} & \omega^{24} & \omega^{30} & \omega^{36} & \omega^{42} \\ \omega^0 & \omega^7 & \omega^{14} & \omega^{21} & \omega^{28} & \omega^{35} & \omega^{42} & \omega^{49} \end{bmatrix} \quad (5.8)$$

Notice that the powers of ω is a different multiple in each row. The multiple is in fact the row index k . But why? This is the speed at which ω goes around the unit circle creating the harmonic at that frequency.

Let us examine each harmonic starting from row 1 noting that row 0 gives $\omega^0 = 1$ and this is just a constant, thus given us the sum of the signal (or DC offset). At row 1

$$\mathbf{F}_1 = [\omega^0 \quad \omega^1 \quad \omega^2 \quad \omega^3 \quad \omega^4 \quad \omega^5 \quad \omega^6 \quad \omega^7] \quad (5.9)$$

Using the fact that multiplication of complex exponentials results in the sum of their angles, the above can be done considering only the unit circle as $\theta = \pi/4$. This is because $N = 8$ divides the circle into 8 parts

with every second octant making a quadrant that intersects with the imaginary and real axis, i.e. the values are either $1, i, -1, -i$ and back to 1. This process is shown in figure 5.3

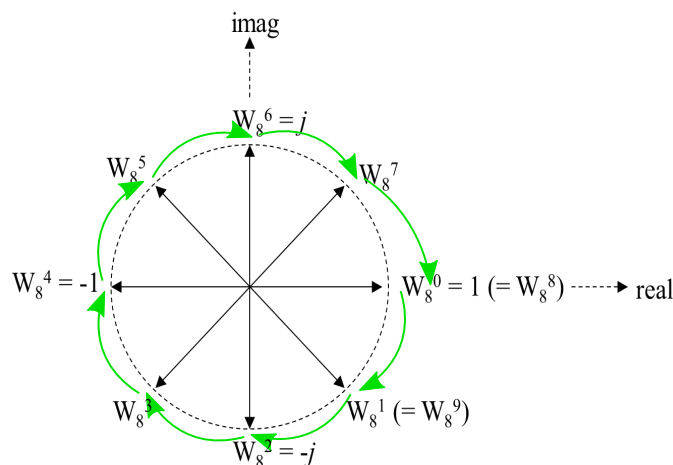


Figure 5.3: For $N = 8$ the circle is divided into 8 parts with every second octant making a quadrant that intersects with the imaginary and real axis, i.e. the values are either $1, i, -1, -i$ and back to 1. Sometimes the symbol j is used as a convention for the imaginary unit i .

Examining the second harmonic on row 2

$$\mathbf{F}_2 = [\omega^0 \ \omega^2 \ \omega^4 \ \omega^6 \ \omega^8 \ \omega^{10} \ \omega^{12} \ \omega^{14}] \quad (5.10)$$

Since $\omega = 0.707 - 0.707i$ for $N = 8$, the second row of \mathbf{F} is

$$[1 + 0.i \ 0 - 1.i \ -1 - 0.i \ 0 + 1.i \ 1 + 0.i \ 0 - 1.i \ -1 - 0.i \ 0 + 1.i]$$

Using the same multiplication property of complex exponentials, the above can be computed as rotation around the unit circle with $\theta = \pi/2$. This is twice the rate as for row 1 with each multiplication resulting with each value being the quadrants that intersects with the imaginary and real axis, i.e. the values are either $1, i, -1, -i$ and back to 1 twice. This is shown in figure 5.4 on the next page.

Examining the second harmonic on row 3

$$\mathbf{F}_2 = [\omega^0 \ \omega^3 \ \omega^6 \ \omega^9 \ \omega^{12} \ \omega^{15} \ \omega^{18} \ \omega^{21}] \quad (5.11)$$

Since $\omega = 0.707 - 0.707i$ for $N = 8$, the third row of \mathbf{F} is

$$[1 + 0.i \ -0.707 - 0.707i \ 0 + 1.i \ 0.707 - 0.707i \ -1 - 0.i \ 0.707 + 0.707i \ 0 - 1.i \ -0.707 + 0.707i]$$

The above can be computed as rotation around the unit circle three times the rate as for row 1 with each multiplication resulting with each value being every third octant. This is shown in figure 5.5 on the following page.

The harmonics share two important properties that make them ideal as basis functions. The harmonics are both orthogonal to each other and of unit magnitude, i.e. they are orthonormal by construction, which are properties that can be easily verified by the reader. This allows harmonics to be used as basis functions of our transform and all we need to do is to compute the dot product with these harmonic functions.

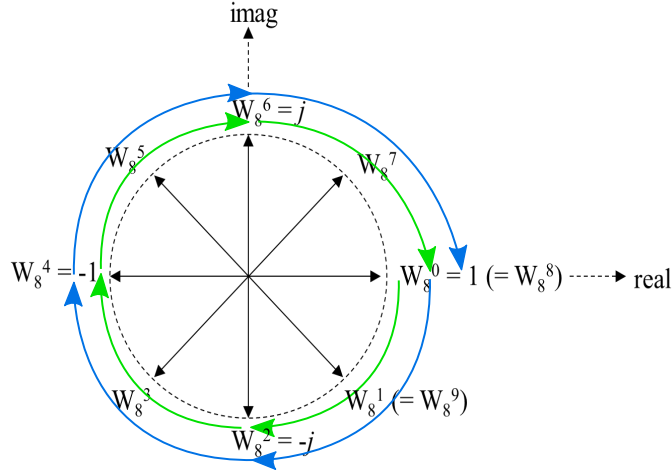


Figure 5.4: Traversing the unit circle at twice the rate as for row 1 shown in figure 5.3 on the previous page with each multiplication resulting with each value being the quadrants that intersects with the imaginary and real axis, i.e. the values are either $1, i, -1, -i$ and back to 1 twice.

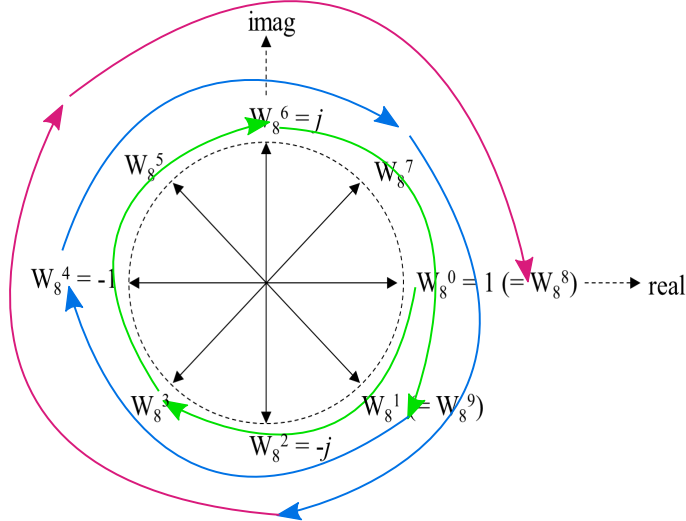


Figure 5.5: Traversing the unit circle at three times the rate as for row 1 shown in figure 5.3 on the preceding page with each multiplication resulting with each value being every third octant.

5.2.4 Discrete Fourier Transform

The discrete Fourier transform (DFT) is the projection of our data (in vector form) onto the harmonic functions we described in the previous section. Since the root of unity ω is fixed and known for the size N . The harmonics of the Fourier matrix F can be predefined. Thus, we simply need to compute the inner product with our data/signal x . This can be viewed as an inner product between two N -vectors, i.e. vectors of dimension N (in a linear algebra sense). For example, vectors representing 3D space would be 3-vectors.

Therefore, the **DFT** $\mathbf{X} = X_k$ of the signal $\mathbf{x} = x_n$ can be defined as

$$X_k = \sum_{n=0}^{N-1} x_n \cdot \omega^{kn}, \quad (5.12)$$

where the N th root of unity is defined as

$$\omega = e^{2\pi i/N}. \quad (5.13)$$

The inverse **DFT** is simply the traversal of the unit circle in the opposite direction

$$x_n = \sum_{k=0}^{N-1} X_k \cdot \omega^{-kn}, \quad (5.14)$$

It is usually more efficient to use the fast Fourier transform (**FFT**) implementation of the **DFT** in practice. This is a highly optimised algorithm for the **DFT** that uses the symmetry in the Fourier matrix \mathbf{F} to reduce the complexity of the algorithm from $O(N^2)$ to $O(N \log_2 N)$.

The **DFT** can reveal hidden harmonic signatures, especially those caused by physical systems, such as sound or motion. In fact, the **DFT** is an ideal transform for signals or data originating from physical sources, since most physical systems have some oscillatory phenomena behind them.

5.3 Principal Component Analysis

Ideally, our data would be represented using the basis set that gives us the most “compact” representation. By compact we mean representing our data with as few basis vectors as possible. This compact representation can only be obtained by identifying the patterns in our data and one way to do this is to compute its principal components. This representation involving principal components is called principal component analysis (**PCA**). A form of **PCA** was first introduced by Pearson [1901] and also known as the Karhunen–Loève Transform.

Consider the extreme examples shown in figures 5.6 on the next page and 5.7 on the following page. The data points in figure 5.6 on the next page has a linear structure, while the data points in figure 5.7 on the following page appears to have three axes or directions as shown by the linear fits in figure 5.7(b).

In these cases, it is clear that we should exploit the linear aspects we can see in the data. If we look at the individual data points that make up data set in figure 5.6 on the next page, we can represent each data

points as a vector $\mathbf{x}_i = \begin{bmatrix} x_i \\ y_i \end{bmatrix}$ and therefore be able to create the data matrix by vertically stacking all s data points \mathbf{x}_i

$$\mathbf{X} = \begin{bmatrix} x_0 & x_1 & x_2 & \dots & x_{s-1} \\ y_0 & y_1 & y_2 & & y_{s-1} \end{bmatrix} \quad (5.15)$$

If we ignore the small “noise” in our data points from figure 5.6 on the following page, our most “compact” representation is that of a line. Therefore, we should be able to represent each point as simply scalings b of a vector \mathbf{u} with the slope corresponding to the line. Thus in theory, we can represent the entire data matrix \mathbf{X} with a new matrix \mathbf{U} of k columns, so that $k \ll s$ and $k = 1$ in our case giving

$$\mathbf{U} = \begin{bmatrix} u_0 \\ v_0 \end{bmatrix} \quad (5.16)$$

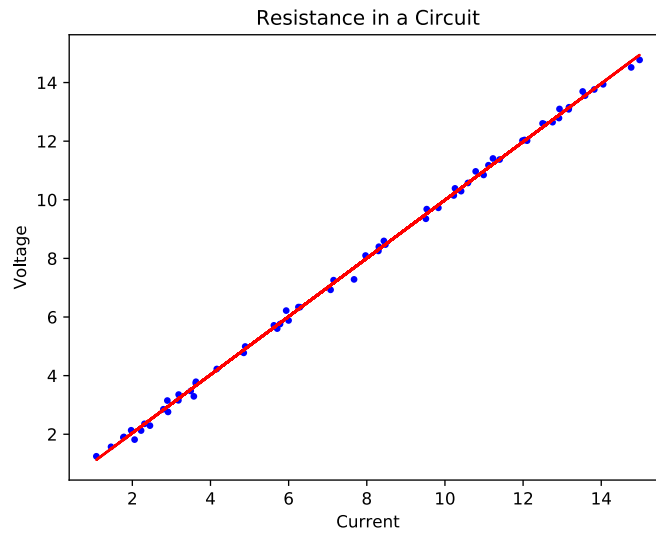


Figure 5.6: Example dataset of 64 data points with an embedded linear direction.

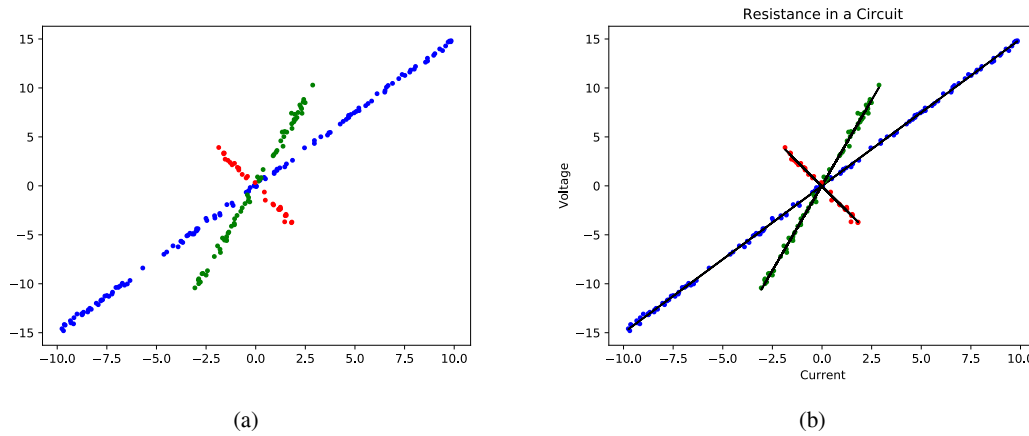


Figure 5.7: Example datasets of 128, 64 and 32 data points with multiple embedded linear directions.

Likewise for the dataset in figure 5.7, we can represent the entire data matrix \mathbf{X} with a new matrix \mathbf{U} of $k = 3$ columns

$$\mathbf{U} = \begin{bmatrix} u_0 & u_1 & u_2 \\ v_0 & v_2 & v_2 \end{bmatrix} \quad (5.17)$$

with each of \mathbf{u}_i having the directions corresponding to the slope of each line. We can then recover each data point in the dataset by creating a linear combination of these \mathbf{u}_i vectors as

$$\mathbf{x}_i = \sum_{i=0}^{k-1} b_i \mathbf{u}_i. \quad (5.18)$$

Notice that here we have reduced the number of columns of our original dataset from s to k . This is in essence the notion of the dimensionality reduction that **PCA** provides. The \mathbf{u}_i vectors are known as eigenvectors and form the principal components. Computing these vectors is based on the fundamental concept of eigen-decomposition.

5.3.1 Eigen-decomposition

Recall that in the chapter on symmetry, we defined symmetry as a property that remains unchanged after a transformation. Eigen-decomposition provides a method to do this with respect to basis vectors of a given dataset. Given a transformation \mathbf{A} of vectors of n dimensions, the goal of eigen-decomposition is to find vectors \mathbf{u} such that

$$\mathbf{A}\mathbf{u} = \lambda\mathbf{u}, \quad (5.19)$$

where λ is a scalar value called the eigenvalue. In other words, these eigenvectors \mathbf{u} are vectors that remain invariant to any rotations induced by transformation \mathbf{A} . The vectors \mathbf{u} do not change direction when \mathbf{A} is applied to them.

In our examples from figures 5.6 on the facing page and 5.7 on the preceding page, these eigenvectors were oriented along the lines shown. Any point in those datasets can be represented by a linear combination of scaled version of the eigenvectors shown in equation (5.18). Now using linear algebra, we can extend the concept to any number of training samples s and points N .

To compute this eigen-decomposition, we can use the singular value decomposition (**SVD**) algorithm that decomposes the matrix \mathbf{A} as

$$\mathbf{A} = \mathbf{U}\mathbf{W}\mathbf{V}^T, \quad (5.20)$$

where \mathbf{W} is a diagonal matrix whose entries are the singular values in descending order that correspond to the eigenvalues. Note that the data matrix should be centered, i.e. $\mathbf{A} = \hat{\mathbf{X}} = \mathbf{X} - \boldsymbol{\mu}$ where $\boldsymbol{\mu}$ is the mean of the training vectors or columns. The matrix \mathbf{U} corresponds to the eigenvectors of the decomposition.

5.3.2 Dimensionality Reduction

In terms pattern recognition, we determine the eigen-decomposition a rectangular ($N \times s$) data matrix $\mathbf{X} = \mathbf{x}_j$ (see algorithm 1). Thus, meaningful variations are obtained for each row in \mathbf{X} that represents the same regions of the data.

Algorithm 1 **PCA** Algorithm [Pearson, 1901, adapted]

- 1: $\mathbf{X} \leftarrow$ dataset
 - 2: $\boldsymbol{\mu} \leftarrow$ mean vector from \mathbf{X} .
 - 3: $\hat{\mathbf{X}} \leftarrow \mathbf{X} - \boldsymbol{\mu}$ ▷ Each column consists of variational points
 - 4: Compute the **SVD** of $\hat{\mathbf{X}}$ to get estimate of \mathbf{U} .
 - 5: **return** \mathbf{U} and λ_i ▷ The **PCA** model
-

The **PCA** produces an eigen-decomposition of the data matrix $\hat{\mathbf{X}}$, where $\hat{\mathbf{X}}$ represents the training data with the mean vector $\boldsymbol{\mu}$ removed. The eigen-decomposition results in a set of eigenvectors $\mathbf{U} = [\mathbf{u}_1, \dots, \mathbf{u}_s] = \mathbf{u}_i$ and eigenvalues λ_i that effectively represent a set of modes that model how each data point varies from the mean data point given the training vectors. One can then project a training vector $\mathbf{S} = [\mathbf{v}_1, \dots, \mathbf{v}_s] = \mathbf{v}_i$ as

$$\mathbf{b}_i = \mathbf{U}^T (\mathbf{v}_i - \boldsymbol{\mu}_i), \quad (5.21)$$

into the variation (**PCA**) model to acquire the variation coefficients b_i . The data vector \mathbf{S} can then be reconstructed as a new vector $\hat{\mathbf{S}} = \hat{\mathbf{v}}_i$ within the constraints of the training set as

$$\hat{\mathbf{v}}_i = \sum_j^k b_{ji} \mathbf{u}_{ji} + \boldsymbol{\mu}_i \approx \mathbf{v}_i, \quad (5.22)$$

where k is the number of modes, so that $k \leq s$ and usually $k \ll s$. The fact that k is the fundamental concept behind dimensionality reduction. In general, only the most significant modes are used, up to a precision of representation $P : 0 < P \leq 1$, for computational efficient and stable reconstructions.

5.3.3 PCA Variants

The robust **PCA** of [Skočaj et al. \[2007\]](#) that can handle missing or corrupted data (hereon referred to as missing data) using binary weights w_{ij} to represent missing or known data for each point in each training surface. In this robust **PCA**, the variations are modelled from the mean of the known data as

$$\boldsymbol{\mu}_i = \frac{1}{\sum_j^N w_{ij}} \sum_j^N w_{ij} \mathbf{x}_{ij}. \quad (5.23)$$

Any detected outliers are replaced by iteratively reconstructed values from a model of the reliable or known data using an expectation maximisation (**EM**) algorithm (see algorithm 2).

Algorithm 2 Iterative Reconstruction **PCA** Algorithm [[Skočaj et al., 2007](#)]

- 1: $\mathbf{X} \leftarrow$ known data.
 - 2: $\mathbf{W} \leftarrow$ binary weights representing missing and known data. ▷ Can accommodate partial data in training
 - 3: $\boldsymbol{\mu} \leftarrow$ weighted mean from known data from equation (5.23).
 - 4: $\hat{\mathbf{X}} \leftarrow \mathbf{X} - \boldsymbol{\mu}$
 - 5: Apply **PCA** on known data in $\hat{\mathbf{X}}$ via algorithm 1. ▷ Initialise the algorithm with the known model
 - 6: $\mathbf{Y} \leftarrow \hat{\mathbf{X}}$
 - 7: **while** not converged **do**
 - 8: E-step: Project known data with the pseudo-inverse of weighted \mathbf{U} . ▷ Element-wise product with \mathbf{W}
 - 9: M-step 1: Reconstruct $\hat{\mathbf{X}}$ with current model.
 - 10: M-step 2: $\mathbf{Y} \leftarrow \hat{\mathbf{X}}$ with missing data replaced by reconstructed values. ▷ Recovers missing data here
 - 11: M-step 3: Re-estimate \mathbf{U} by **PCA** on \mathbf{Y} .
 - 12: **end while**
 - 13: **return** \mathbf{U} and λ_i ▷ The robust shape model
-

The spatially weighted **PCA** of [Thomaz et al. \[2010\]](#)¹ is simpler to implement than the robust **PCA** as can be seen from comparing algorithms 2 and 3. The weights

$$\mathbf{w}_i = [\sqrt{w_1}, \sqrt{w_2}, \dots, \sqrt{w_N}], \quad (5.24)$$

are determined from regions that of the data that needs to be contoured and are applied to all training samples via the correspondences present. To reduce computation complexity in the projection stage, only the first $k \leq s$ need to be used.

The spatially weighted **PCA** of [Thomaz et al. \[2010\]](#) has important distinctions to the temporally and spatially weighted **PCAs** proposed by [Skočaj et al. \[2007\]](#). The temporally weighted **PCA** weights each

¹See also the related work of [Thomaz and Giralaldi \[2010\]](#).

Algorithm 3 Spatially Weighted PCA Algorithm [Thomaz et al., 2010]

-
- 1: $\mathbf{X} \leftarrow$ dataset.
 - 2: $\mathbf{w}_i \leftarrow$ square root of the weights representing regions. ▷ Weights represent important regions
 - 3: $\boldsymbol{\mu} \leftarrow$ weighted mean from equation (5.23).
 - 4: $\hat{\mathbf{X}} \leftarrow \mathbf{X} - \boldsymbol{\mu}$
 - 5: Multiply each row of $\hat{\mathbf{X}}$ with \mathbf{w}_i to get \mathbf{Y} . ▷ Weight each corresponding point
 - 6: Apply PCA on \mathbf{Y} via algorithm 1.
 - 7: **return** \mathbf{U} and λ_i ▷ The focused shape model
-

training shape (or column of the training matrix), which is suitable for handling unreliable or low quality training shapes as a whole. The spatially weighted PCA of Skočaj et al. [2007] is a general scheme solved using an EM algorithm for weighting arbitrary points in any of the training shapes and not just each corresponding point (or row of the training matrix) as with the spatially weighted PCA of Thomaz et al. [2010], so that \mathbf{w} is a matrix and not a vector. In the spatially weighted PCA of Thomaz et al. [2010], entire regions maybe weighted and their variations from the mean shape scaled as desired. This weighting of a corresponding point for all training surfaces such as (5.24) is not possible with the spatially weighted PCA of Skočaj et al. [2007] as the weightings are lost from the eigenvectors in the process of removing the weighted mean from the data matrix².

The last consideration when using the weighted PCA is that it cannot accommodate missing data in the same way as the robust PCA. This means that zero-valued weights cannot be used, but can be handled by using very small values (e.g. 1×10^{-6}) instead.

5.4 Radon Transform

Svalbe [1989]

5.5 Wavelet Transforms

²Equations (7) and (8) of the work of Skočaj et al. [2007] separates the weights from the eigenvectors and so no weights (such as (5.24)) are directly encoded in the resulting eigenvectors leading to no weighted dimensionality reduction normally afforded to us by the PCA.